



**HAL**  
open science

## **Anthropogenic versus natural control on lacustrine sediment yield records from the French Massif Central**

Léo Chassiot, Anaëlle Simonneau, Emmanuel Chapron, Christian Di Giovanni

### ► **To cite this version:**

Léo Chassiot, Anaëlle Simonneau, Emmanuel Chapron, Christian Di Giovanni. Anthropogenic versus natural control on lacustrine sediment yield records from the French Massif Central. *Quaternary International*, 2022, 636, pp.154-166. 10.1016/j.quaint.2021.12.012 . insu-03567916

**HAL Id: insu-03567916**

**<https://insu.hal.science/insu-03567916v1>**

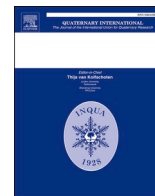
Submitted on 12 Feb 2022

**HAL** is a multi-disciplinary open access archive for the deposit and dissemination of scientific research documents, whether they are published or not. The documents may come from teaching and research institutions in France or abroad, or from public or private research centers.

L'archive ouverte pluridisciplinaire **HAL**, est destinée au dépôt et à la diffusion de documents scientifiques de niveau recherche, publiés ou non, émanant des établissements d'enseignement et de recherche français ou étrangers, des laboratoires publics ou privés.

Contents lists available at [ScienceDirect](https://www.sciencedirect.com)

Quaternary International

journal homepage: [www.elsevier.com/locate/quaint](http://www.elsevier.com/locate/quaint)

## Anthropogenic versus natural control on lacustrine sediment yield records from the French Massif Central

Léo Chassiot<sup>a,b,\*</sup>, Anaëlle Simonneau<sup>b</sup>, Emmanuel Chapron<sup>b,c</sup>, Christian Di Giovanni<sup>b,1</sup>

<sup>a</sup> Université Laval, Département de Géographie, 2405 rue de la Terrasse, G1V 0A6, Québec City, QC, Canada

<sup>b</sup> Université d'Orléans, CNRS UMR 7327 ISTO, BRGM, 1a rue de la Ferronnerie, 45071 Orléans Cedex 2, France

<sup>c</sup> Université Toulouse 2 Jean-Jaurès, CNRS UMR 5602 GEODE, Allée A. Machado, 31058, Toulouse, France

### ARTICLE INFO

#### Keywords:

Soil erosion  
Quantitative organic petrography  
Land-use change  
French Massif central  
Agro-pastoral activities  
Lake sediments

### ABSTRACT

A quantitative assessment of historical sediment yields (SY) was performed using sediment budgets from lacustrine records located in the Mont Dore and Cézallier volcanic provinces (French Massif Central). A source-to-sink approach combining hydro-acoustic images, organic geochemistry (Rock-Eval and quantitative organic petrography) and radiocarbon dating of sediment cores has been adopted on three lake-catchment systems, namely Pavin, Chauvet and Montcineyre. SY was estimated from the quantification of red Amorphous Particles (rAP), a terrigenous organic tracer identified in both soils and sediments. Historical SY range between 3 and 320 t km<sup>-2</sup>.yr<sup>-1</sup>, which is comparable to the magnitude reached in other European lake-based SY records in similar geographical and climatic settings. Comparison of recent SY with predicted values of soil erosion rates from the RUSLE2015 model highlights large differences linked to scale differences between the model at plot scale and lake-based SY reflecting erosion export from the catchment to the lake. In this sense, the role of peatlands as sediment traps within two studied catchments must be considered to explain the large differences between modelled soil erosion rates and reconstructed SY data. SY differences between sites can be firstly attributed to morphology, size and lithology of the catchments as well as to vegetation cover whereas fluctuations reconstructed for each record seem to be mainly related to human-induced land use management. Historical SY from Chauvet and Montcineyre synchronously recorded two events in 850 CE and 1450 CE, respectively. The first marked the rise of SY to their maxima following land-use changes in the catchments. Nearby palaeoenvironmental records from Lake Aydat, Chambedaze peatland, and Espinasse marsh suggest this rise was consecutive to intensification of agro-pastoral activities recorded at regional scale. The second event followed a land-use shift characterized by a ten to fifteen-fold decrease in SY values. The driver remains unclear but could be possibly related to historical events causing a demographic decline (i.e., the Black Plague and/or the Hundred Years War) and/or cultural adaption in response to the onset of the Little Ice Age. Overall, both records suggest erosion in the area has been historically more susceptible to human-induced land use change rather than to precipitation and temperature changes induced by climate variability of the past millennium.

### 1. Introduction

Soil erosion is a worldwide challenge for countries facing landscape degradation. Hence, recent studies reporting pedogenesis rates inferior to erosion rates (Verheijen et al., 2009; Panagos et al., 2015) and/or predicting higher soil erosion rates as a result of ongoing climate change (Nearing et al., 2004) have led to the development and implementation of sustainable management policies to prevent land degradation and

ensure soil and water quality as well as food security (e.g., European Commission, 2006; Kuhlman et al., 2010; Lal et al., 2011; Garbrecht et al., 2014). Soil erosion is a natural phenomenon with its magnitude related to biological, physical and chemical properties of soils, relief, earthquakes, land cover and climate variability (Syvitski and Milliman, 2007; Verheijen et al., 2009 and references therein). However, the global spread of human activities, including deforestation, agriculture and urbanization, have affected ecosystem stability so much that

\* Corresponding author. Université Laval, Department of Geography, 2405 rue de la Terrasse, G1V 0A6, Quebec City, QC, Canada.

E-mail address: [leo.chassiot.1@ulaval.ca](mailto:leo.chassiot.1@ulaval.ca) (L. Chassiot).

<sup>1</sup> Deceased.

<https://doi.org/10.1016/j.quaint.2021.12.012>

Received 26 September 2018; Received in revised form 6 December 2021; Accepted 15 December 2021

1040-6182/© 2021 Elsevier Ltd and INQUA. All rights reserved.

humans are nowadays recognized as major geological agents for soil erosion and sediment transfer (Dearing and Jones, 2003; Yang et al., 2003; Syvitski and Milliman, 2007; Simonneau et al., 2013a; Foucher et al., 2014; Bajard et al., 2017; Brisset et al., 2017).

Developing sustainable policies for the future requires knowledge about ecological trajectories that ecosystems have followed in the past. Long-term assessment of interactions between human societies, their environment and climate is thus of primary interest to establish and quantify relationships between factors leading to land degradation by water erosion (Dearing et al., 2006, 2010). Instrumental data covering the last century are too short to provide sufficient information, especially as the modern era is facing unprecedented changes in global population density under a rising temperature regime. Conversely, lake sediments can provide a long-term (i.e., Holocene) environmental history under human and climate pressures (Arnaud et al., 2016; Mills et al., 2017). More specifically, lake sediment budgets can be used to document the evolution of sediment yield (SY) in their catchment (Einsele and Hinderer, 1998; Verstraeten and Poesen, 2002; Dearing and Jones, 2003). In this sense, various approaches attempting at reconstructing historical SY from lake sediment budgets have been successfully conducted in areas covering a wide range of geological, geographical, historical and climate settings (e.g., Dearing et al., 1987; Gaillard et al., 1991; O'Hara et al., 1993; Desloges, 1994; Evans, 1997; Zolitschka, 1998; Lamoureux, 2002; Anselmetti et al., 2007; Enters et al., 2008; Breuer et al., 2013; Foucher et al., 2014; Bajard et al., 2017; Barreiro-Lostres et al., 2017), including volcanic lakes from the French Massif Central (FMC), as demonstrated by Gay and Macaire (1999), Degeai and Pastre (2009), and Macaire et al. (2010).

In the FMC, successive volcanic eruptions and Quaternary glaciations have shaped a mid-altitude landscape with contrasted lacustrine settings such as maar lakes, glacial lakes and volcanic dam lakes. More recently, attention was given to several lakes located in the northern part of the FMC where up to now, Holocene records were only collected in lakes Chambon (Gay and Macaire, 1999), Pavin (Chassiot et al., 2018) and Aydat (Lavrieux et al., 2013a; Miras et al., 2015). A comparison between these records has shown regional discrepancies attributed to local human impacts. For the last millennium, human activities, climatic variations, and their influence on sedimentary processes remains faintly understood, except for Lake Pavin (Chassiot et al., 2018). Moreover, quantitative aspects of erosion and sediment yield have not been addressed yet. This article aims at using data collected between 2010 and 2015 from lakes Pavin (Chapron et al., 2010, 2012; Chassiot et al., 2016a, 2018), Chauvet, and Montcineyre (Chapron et al., 2012; Chassiot et al., 2016b) to document interplays between natural and anthropogenic factors on terrestrial fluxes. By combining hydro-acoustic surveys and organic geochemistry (Rock-Eval pyrolysis coupled to quantitative

organic petrography) on soils and sediment cores, we applied a source-to-sink method developed by Simonneau (2012) to reconstruct historical SY. A comparison with nearby lacustrine records and historical data is finally proposed to include this study into a regional framework and to discuss the respective roles of natural and anthropogenic factors on timing and magnitude of SY fluctuations. An evaluation of geomorphic processes occurring in the catchments is then proposed by comparing SY with both modern soil erosion rates from the Revised Universal Soil Loss Equation (RUSLE2015), available at European scale at a 100 x 100 m resolution (Panagos et al., 2015), and historical lake-based records of SY from similar geographical settings.

## 2. Regional setting

### 2.1. Geographical and climatic context

The sites studied are located in the FMC at the boundary between the Mont-Dore and the Cézaillier volcanic provinces in central France (Fig. 1A, Table 1). In this mid-altitude area (1150–1450 m a.s.l.), precipitation originating from the Atlantic Ocean ranges between 1200 and 1600 mm with frequent snowfall during winters (Stebich et al., 2005).

### 2.2. Limnogeological settings

Lake Pavin (45.4957°N; 2.8878°E) is a 7000-yr old, 92-m deep maar lake (surface area: 0.44 km<sup>2</sup>) with a small and steep catchment (area: 0.36 km<sup>2</sup>) today covered by dense forests (Fig. 1B). Sediments in Lake Pavin are deposited according to three sedimentary environments (Chapron et al., 2010, 2016): the littoral in the northern side above a water depth of 26 m, the plateau in the northern side between 26 and 45 m, and the deep flat central basin below 92 m (Fig. 2). A series of

**Table 1**  
Morphological setting of studied lakes.

|  | Pavin       | Chauvet    | Montcineyre  |
|--|-------------|------------|--------------|
| Type of lake                                 | Maar        | Maar       | Volcanic dam |
| Altitude (m above sea level)                 | 1197        | 1161       | 1182         |
| Max depth: D (m)                             | 92          | 63         | 20           |
| Area: A (km <sup>2</sup> )                   | 0.44        | 0.52       | 0.39         |
| Catchment area: S (km <sup>2</sup> )         | 0.36        | 1.27       | 1.38         |
| Catchment slopes (min - mean - max; degrees) | 0 - 27 - 73 | 0 - 8 - 41 | 0 - 10 - 56  |
| Lake/Catchment ratio: A/S                    | 1.22        | 0.41       | 0.28         |
| Aspect ratio: D/√(Ax100) <sup>a</sup>        | 13.87       | 8.73       | 3.20         |

<sup>a</sup> Modified according to Rioual (2002).

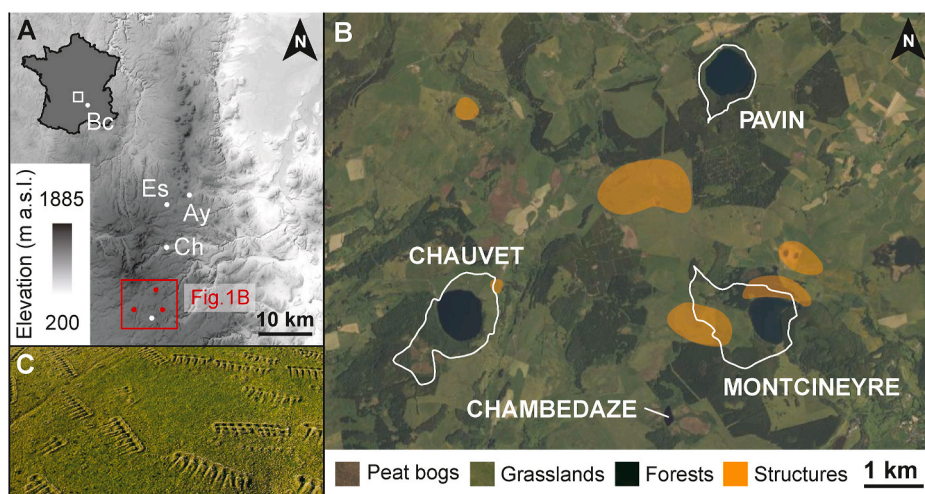


**Fig. 1.** (A) Digital Elevation Model of the French Massif Central (source: [www.geoportail.fr](http://www.geoportail.fr)) displaying the location of the sites studied (red points) along with regional studies referenced in the text (white points). Ay: Lake Aydat, Bc: Lake Bouchet, Ch: Lake Chambon, Es: Espinasse peat marsh. (B) Aerial photography of the studied area (red box in A) displaying vegetation cover and location of archaeological structures around the catchments of the Lakes Pavin, Chauvet and Montcineyre (white lines) (source: <https://www.geoportail.gouv.fr/>). (C) Aerial photography (courtesy of Francis Cormon) showing archaeological (i.e. comb-shaped and half-buried) structures associated to regional pastoral activities in the past. (For interpretation of the references to colour in this figure legend, the reader is referred to the Web version of this article.)

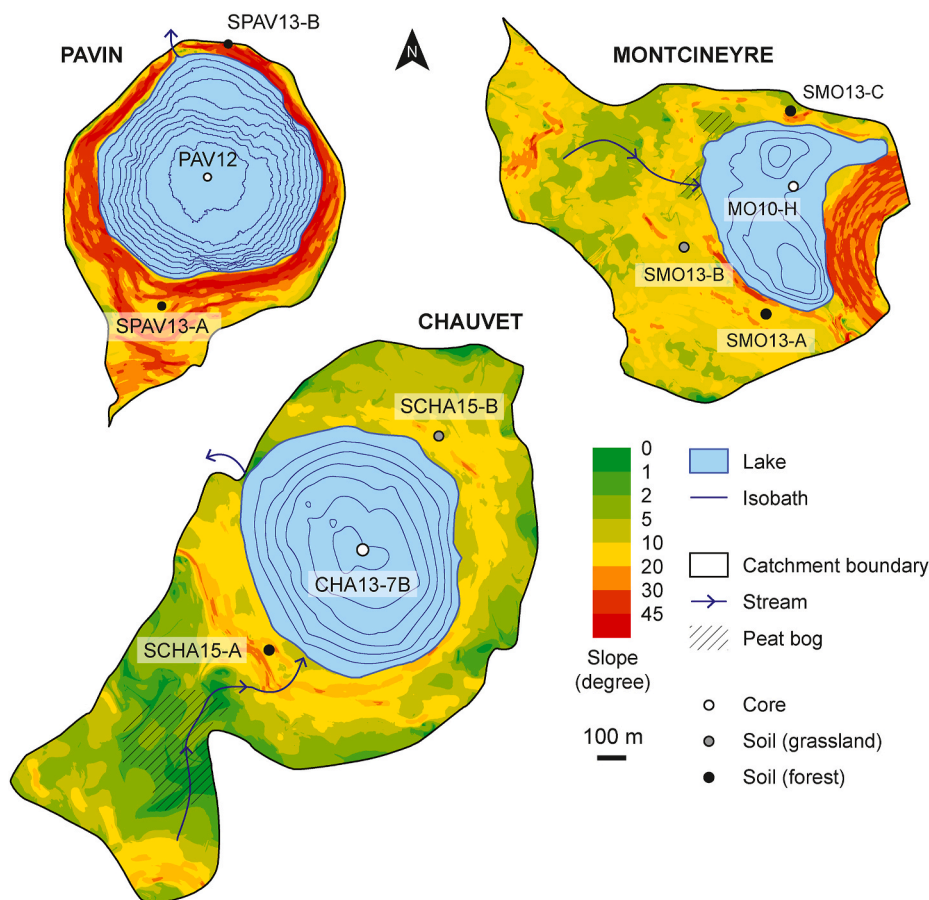


Fig. 2. Slope maps of catchment areas, lake bathymetries, and location of sediment cores (white dots) and soil samples (black dots) of the sites studied in the French Massif Central. Isobaths intervals are of 10 m for lakes Pavin and Chauvet and of 5 m for Lake Montcineyre (Chassiot et al., 2016b).

radiocarbon-dated sediment cores collected in these different environments show that sedimentation rates in the littoral and the plateau is much lower than in the deep basin (Chapron et al., 2010, 2012, 2016; Chassiot et al., 2016a, 2016b). Additionally, steep subaquatic slopes in Lake Pavin are preventing the accumulation of sediments and are frequently shaped by active canyons. These canyons are focusing clastic sediment supply originating from littoral environments and the drainage basin directly into the deep central basin where a lacustrine drape was evidenced on 3.5 kHz hydro-acoustic profiles (Chapron et al., 2010). These canyons are draining small subaerial streams and gullies identified at the steep inner slopes of the crater rim (Thouret et al., 2016).

Lake Chauvet (45.4593°N; 2.8311°E) is a 63 m deep maar lake (surface area: 0.52 km<sup>2</sup>) where the presence of moraines within and around the lake suggests an eruption during the Last Glacial Era (Juvigné, 1992; Chapron et al., 2012; Chassiot et al., 2016b). Its catchment area (1.27 km<sup>2</sup>) is covered by grasslands in the northeastern part and by forests in the southwestern part (Fig. 1B). The lake is currently fed by a small stream flowing from a plateau covered by a peat bog (Fig. 2).

Lake Montcineyre (45.4592°N; 2.8960°E) has a crescent shape (surface area: 0.39 km<sup>2</sup>) resulting from the damming of the valley by the Montcineyre volcano that erupted a few centuries before Lake Pavin (Juvigné et al., 1996). The bathymetric map displays two sub-basins both reaching 19 m depth (Chassiot et al., 2016b). The catchment area (1.38 km<sup>2</sup>) can be parted into the steep wooded flanks of the volcano to the east and a valley in the west where a small stream flows between grasslands and forests (Figs. 1B and 2).

### 2.3. Historical human settlements

Early human activities are documented in the area since the Neolithic (Perpère, 1979; Daugas and Raynal, 1989; Miras et al., 2004; 2015). Few historical information is available for the last millennium but many archaeological remains can be observed on aerial photographs (Fig. 1B). Among them, many comb-shaped half-buried structures indicative of pastoral activities are scattered around the three investigated sites (Fig. 1C) (Fournier, 1962; Fel, 1984; Surmely et al., 2009). The lack of archaeological and historical studies on these structures however impedes an accurate comprehension of the past rural demography. Their census hence does not reflect the intensity of human impact at local scale. Moreover, the chronological framework about their occupation remains unclear, with a seasonal or year-round use from the XI<sup>th</sup> and the XIX<sup>th</sup> century (Fournier, 1962; Surmely, personal communication). During the past millennium, human-induced landscape openings were inferred from pollen records of lakes Chambadaze (Guenet and Reille, 1988) and Pavin (Stebich et al., 2005; Chassiot et al., 2018) (Fig. 1B). In the sedimentary record of Lake Montcineyre, the identification of faecal biomarkers of cows since 1275 CE demonstrated the uninterrupted presence of livestock husbandry within the catchment (Zocatelli et al., 2017). Human occupation in the area during the last millennium was thus mainly related to agro-pastoral activities having required landscape opening. Rural exodus initiated in the late XIX<sup>th</sup> century then caused a demographic decline. Since then, the last significant human impact on these rural landscape is the afforestation with spruce (*Picea abies*), notably within the catchments of lakes Pavin and Montcineyre (Stebich et al., 2005; Chassiot et al., 2018) (Fig. 1B).

### 3. Materials & methods

A source-to-sink approach, originally developed by Simonneau (2012), was applied to reconstruct historical SY for the three lake-catchment systems (Fig. 3). Field and analytic strategies consisted in (1) hydro-acoustic images obtained with a Knudsen™ high-resolution seismic reflection device equipped with a frequency modulator of 4, 12 and 200 kHz (Chapron et al., 2012, 2016; Chassiot et al., 2016a, 2016b); (2) multi-proxy analyses of sediment cores and soils profiles, including dry bulk density (DBD), Rock-Eval 6 pyrolysis (RE, Behar et al., 2001; Disnar et al., 2003; Sebag et al., 2006b) and quantitative organic petrography (QOP, Sebag et al., 2006a; Graz et al., 2010; Simonneau et al., 2013a, 2013b, 2014; Chassiot et al., 2018; Allen et al., 2020); and (3) radiocarbon dating of sediment cores (Chassiot et al., 2016b, 2018).

#### 3.1. Hydro-acoustic surveys

Hydro-acoustic images are widely used to document the geometry of sediment infills and to locate suitable coring sites. In this study, seismic-to-core correlations were used to extend chronological and geochemical information inferred from the multi-proxy analysis of a sediment core to the lake basin scale (e.g., Anselmetti et al., 2007; Breuer et al., 2013). Otherwise, the assessment of SY could be less accurate and often requires multiple cores and analyses (e.g., Lamoureux, 2002; Macaire et al., 2010). Within lakes Chauvet and Montcineyre, 12 kHz hydro-acoustic profiles recorded using a KNUDSEN™ sounder were used to determine the lake surface area within which sediment yields can be assessed. In Lake Pavin, gas-rich sediments limited imagery of infills in the deep basin. However, the use of a 3 kHz acoustic source allowed to image the upper meter of sediments corresponding to diatomaceous sediments (Fig. 4, Chapron et al., 2010). Sediment yields derived from core PAV12, collected in the center part of this deep basin, were thus assessed using the 90 m isobath.

#### 3.2. Bulk geochemistry (Rock-Eval 6)

Rock Eval pyrolysis provides a quantitative and qualitative assessment of organic matter through the following parameters: (i) Total Organic Carbon (TOC) expressed in percentage (%), (ii) Hydrogen Index (HI = S2/TOC) expressed in mg.HC.gTOC<sup>-1</sup> where S2 corresponds to the volume of hydrocarbons (HC) formed during thermal pyrolysis of the sample, (iii) Oxygen Index (OI = S3/TOC) expressed in mgCO<sub>2</sub>.gTOC<sup>-1</sup> where S3 corresponds to the CO<sub>2</sub> yield during thermal breakdown of hydrogen, and (iv) TpS2 which corresponds to the maximal temperature reached during pyrolysis of S2.

#### 3.3. Quantitative organic petrography (palynofacies)

QOP was performed to identify and quantify the composition of the organic fraction (Graz et al., 2010). The process includes the destruction of mineral fractions after applying hydrochloric and hydrofluoric acids on 1 cm<sup>3</sup> of sediment, after being dried at 40 °C for a week to assess the DBD. Following Graz et al. (2010), the QOP requires the addition of an internal standard (*Cupressus* sp. pollen) before identification and quantification of each particle according to shape, colour and reflectance (Combaz, 1964) using a transmitted and reflected light microscope. A minimum counting of 500 points was performed per sample to statistically reflect the abundance of each type of particles. The calculation of concentrations in mg per g of sediment was obtained using mean particle density published by Graz et al. (2010). This analysis was performed for each radiocarbon-dated sediment sample retrieved from records previously described by Chassiot et al. (2016b) for lakes Chauvet and Montcineyre and by Chassiot et al. (2018) for Lake Pavin, as well as for each soil sample collected under grassland, deciduous and coniferous forests (Fig. 2). The characterization and the origin of each particle relies on the study of Di Giovanni et al. (1998), Sebag et al. (2006a), Graz et al. (2010) and Simonneau et al. (2013a, 2013b). In this study, we focused on three major types of particles according to their provenance (terrestrial vs. aquatic): (i) Red amorphous particles (rAP) usually defined as the

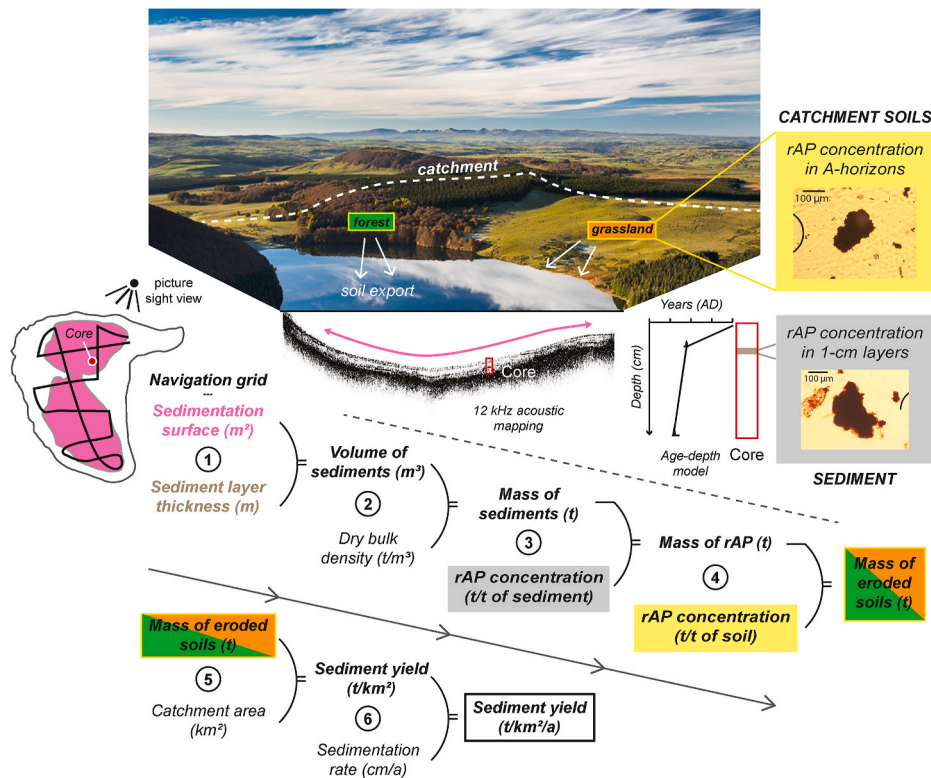


**Fig. 3.** Schematic outline detailing the methodology used to reconstruct sediment yield from quantification of red Amorphous Particles (rAP) in soils (yellow box) and sediments (grey box) at our sites studied in the French Massif Central, modified from Simonneau (2012). A sedimentation surface inferred from sub-bottom hydro-acoustic mapping was used to calculate a volume of sediment (1). This volume was converted into a mass (2) using the dry bulk density. A mass of rAP (3) was obtained using the rAP concentration in sediments. The rAP concentrations calculated for forested and grassland soils were then used to infer an equivalent amount of eroded soils (4), that was converted into sediment yield using the catchment area (5) and the sedimentation rate (6). (For interpretation of the references to colour in this figure legend, the reader is referred to the Web version of this article.)

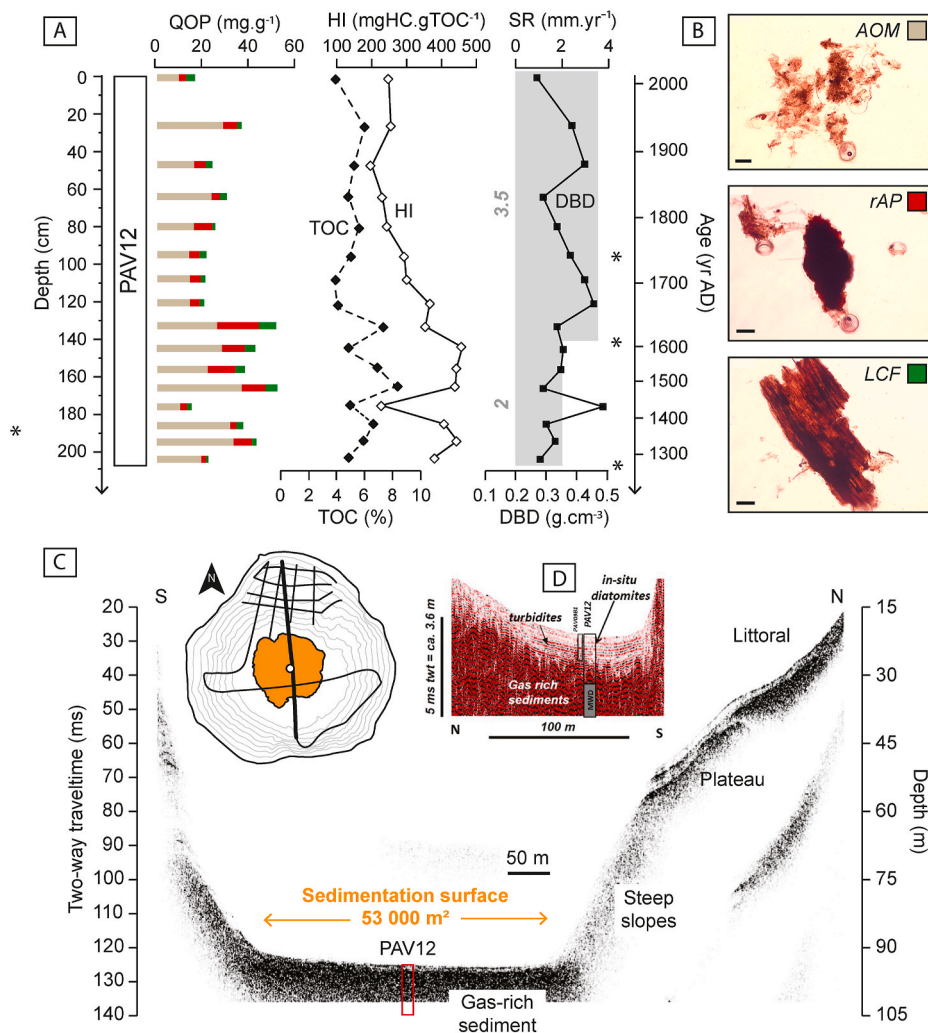


**Fig. 4.** (A) Organic signatures and chronological framework for core PAV12 from Lake Pavin (French Massif Central). Asterisks indicate age controls. QOP: Quantitative Organic Petrography. TOC: Total Organic Carbon, HI: Hydrogen Index, DBD: Dry Bulk Density, SR: Sedimentation Rate. (B) Photomicrographs displaying organic compounds. AOM: Amorphous Organic Matter (primary production), rAP: red Amorphous Particles (soils), LCF: Ligno-cellulosic Fragments (upland vegetation). Black bars correspond to 50 μm. (C) 12 kHz hydro-acoustic image of a north-south profile across Lake Pavin displaying gas-rich sediments in the deep flat basin and limited sedimentary cover within littoral and plateau sedimentary environments. Map of sedimentation surface colored with core (white dot) and seismic lines (black line). (D) 3.5 kHz hydro-acoustic image (Chapron et al., 2010) showing a draping geometry (diatomite) over gas-rich sediments. (For interpretation of the references to colour in this figure legend, the reader is referred to the Web version of this article.)

result of pedogenesis process; (ii) Ligno-cellulosic fragments (LCF), a phytoclast inherited from higher plants and showing variable degradation states, from transparent to degraded; and (iii) brownish amorphous organic matter (AOM) with diffuse edges, typical of aquatic production resulting from the degradation of phytoplanktonic biomass.

### 3.4. Calculation of sediment yields

While AOM was identified in lake sediments only, the presence of LCF and rAP in both soil horizons and sediments were used to develop a source-to-sink approach to quantify terrigenous fluxes (Simonneau et al., 2013a, 2013b, 2014; Foucher et al., 2014; Chassiot et al., 2018; Allen et al., 2020). The quantification of rAP within both lake sediments and topsoil A-horizons allows to convert the concentration of rAP measured in lake sediments into the mass of eroded soil transported and stored to the lake (Fig. 3). The A-horizons were used as references because of their exposure to subaerial erosion and runoff, different from litter horizons that promote infiltration. The collection of soils from various vegetation cover allows reconstructing the mass of eroded soils for two endmembers: a catchment dominated by grassland cover, or dominated by deciduous forests (Fig. 3). Modern coniferous forests were not considered for historical reconstructions. Organic terrigenous signals recorded in lake sediments are therefore a mix of both grassland and forest organic soil horizons. The resulting sedimentary record of eroded soils thus averages the spatial and temporal variations of vegetation cover at the catchment scale. SY, expressed in  $t.km^{-2}.yr^{-1}$ , were

calculated by dividing the mass of eroded soils (in t) by the catchment size (in  $km^2$ ) and the sedimentation rate inferred from age-depth models (in  $cm.yr^{-1}$ ) (Fig. 3).

Because reconstructing SY from lake sediments may be complex if considering too many parameters and sediment sources, several authors simplified the calculation by assuming that overestimating some parameters are counterbalanced by underestimating others (e.g., Zolitschka, 1998). In this sense, our source-to-sink approach lacks of error estimates relative to the accuracy of hydro-acoustic surveys, the spatial representativeness of samples, and the analytical precision (e.g., Evans and Church, 2000; Verstraeten and Poesen, 2002). However, since we considered lake surface areas smaller than total lake areas, SY reconstructions should be regarded as minimum values.

## 4. Results

### 4.1. Soils

The coupling between a temperate climate and young volcanic bedrocks has led to the formation of cambisols and andosols in our study area (Quantin, 2004). At the catchment scale, soil classification is related to vegetation cover, namely (1) grassland where shallow soils display the horizon A over weathered bedrock (horizon C); and (2) forests where thick soils display a succession of litter horizons (OL, OF and OH) over horizon A and altered bedrock.

As summarized in Table 2, horizons from grassland soils are

characterized by: (1) TOC values between 14.2 and 2.2%, showing a decrease with depth, (2) a constant mean TpS2 around  $473 \pm 1$  °C for all depths, (3) low HI values varying from 225 to 335 mgHC.gTOC<sup>-1</sup>, and (4) an increasing OI with depth from 223 to 256 mgCO<sub>2</sub>.gTOC<sup>-1</sup>. Similar observations can be made for horizons A and C from forested soils (Table 2). However, litter horizons show a mean TOC of  $41.6 \pm 0.5\%$  in OL layers with a decreasing trend in lower horizons (mean TOC values equal to  $32.5 \pm 4\%$  for OF layers and to  $20.6 \pm 5\%$  for OH layers). Litter horizons are in addition characterized by lower mean TpS2 values ( $405 \pm 15$  °C) than in horizon A samples where it reached  $470 \pm 1$  °C (mean TpS2 values  $370 \pm 5$  °C for OL layers,  $390 \pm 30$  °C for OF layers, and  $455 \pm 15$  °C for OH layers). OF and OH layers also record maxima of HI with values of up to 625 mgHC.gTOC<sup>-1</sup> (mean HI values  $390 \pm 90$  mgHC.gTOC<sup>-1</sup> for OL layers,  $445 \pm 130$  for OF layers, and to  $430 \pm 115$  for OH layers). The distribution of RE parameters within the studied soils are in agreement with former observations of organic matter dynamics in soils and reflect pedogenesis processes (e.g., Di Giovanni et al., 1998; Disnar et al., 2003; Sebag et al., 2006b; Bajard et al., 2017).

The quantification of organic particles from soil horizons sampled under different vegetation covers shows a higher amount of lignocellulosic fragments (LCF) in top-soil horizons (OL, OF, OH) with a decreasing trend towards deeper horizons (A- and C-horizons) (Table 2). The concentration of LCF is generally higher in forested soils. Red amorphous particles (rAP) are also abundant in topsoil organic horizons, but the highest amount is recorded in OH and/or A-horizons. Like for LCF, the rAP content is higher in forested soils than in soils sampled under grassland. In the pedogenesis process, these particles result of the decay of LCF buried in deeper horizons. Overall, these results confirm that both LCF and rAP are products of the decay of leaf remains during pedogenesis (Di Giovanni et al., 1998; Sebag et al., 2006a). The identification of LCF and rAP in A-horizons sampled under grasslands suggests either that grass or shrubs may also produce these types of

particles, or that their presence is a heritage from ancient forests pre-dating human activities in the catchments.

## 4.2. Lake sediments

### 4.2.1. Lake Pavin

A 7000-yr record (core PAV12, Fig. 2) collected in 2012 in the central part of the deep basin (Chassiot et al., 2016a, 2018) displays two diatomaceous and organic-rich units separated by one major Mass-Wasting Deposit (MWD). The upper unit of core PAV12 covers the last 700 years with a SR ranging from 2 to 3.5 mm.yr<sup>-1</sup> and DBD ranging between 0.23 and 0.45 g cm<sup>-3</sup> (Chassiot et al., 2018) (Fig. 4A). TOC varies between 4 and 8% and HI values between 200 and 460 mgHC.gTOC<sup>-1</sup>. QOP shows a prevalence of amorphous organic matter (AOM) typical of primary productivity with limited terrigenous input mainly composed of rAP and LCF (Fig. 4A).

Gas-rich sediments impeded to map the geometry of deposits within the deep basin (Chapron et al., 2010, 2012, 2016) (Fig. 4B). For this study, the sedimentation surface representative for the core PAV12 chronology corresponds to the surface area covered by the deep and flat central basin delimited by the 90 m isobath (Fig. 4C). The reconstruction of SY for Lake Pavin focuses on the upper 2 m of core PAV12 covering the last 700 years (i.e., the time after deposition of the MWD) documented in Chassiot et al. (2016a, 2016b, 2018) with a surface area of 53, 000 m<sup>2</sup>. This area does not include shallower environments (i.e. the plateau and the littoral) where SR are significantly lower than the deep basin (Chapron et al., 2016; Chassiot et al., 2016a). Accordingly, the limited amount of sediments deposited on these shallower environments over the past 700 years make them negligible compared to the deep basin. As no grassland soils are currently present in the catchment, the rAP content of the soil SMO13-2 (Fig. 2, Table 2) was chosen for picturing historical SY in a catchment where grasslands used to exist

**Table 2**

Organic signatures of soil horizons sampled under grassland and forest cover around the three studied lakes in the French Massif Central (see locations on Fig. 2). Bold values correspond to rAP content of horizons A (organo-mineral horizon) used as reference material for each catchment to reconstruct historical SY. Organic horizons are defined from top to bottom as litter (OL), fragmented (OF), and humus (OH).

| Location     |          |                              |         | Rock-Eval  |         |           |   |   | Organic petrography            |                                |
|--------------|----------|------------------------------|---------|------------|---------|-----------|---|---|--------------------------------|--------------------------------|
| Site         | Soil     | Vegetation                   | Horizon | Depth (cm) | TOC (%) | TpS2 (°C) | Hydrogen Index (mgHC.gTOC <sup>-1</sup> ) | Oxygen Index (mgCO <sub>2</sub> .gTOC <sup>-1</sup> ) | LCF (mg.g soil <sup>-1</sup> ) | rAP (mg.g soil <sup>-1</sup> ) |
| PAVIN        | SPAV13-A | Deciduous + Coniferous trees | OL      | 0–2        | 41.6    | 371       | 488                                       | n.a.  | 52.7                           | 7.6                            |
|              |          |                              | OF      | 5–7        | 34.7    | 427       | 625                                       | n.a.  | 22.6                           | 16.9                           |
|              |          |                              | OH      | 8–9        | 23.8    | 439       | 572                                       | n.a.  | 7.9                            | 39.9                           |
|              |          |                              | A       | 10–20      | 11.5    | 467       | 510                                       | n.a.  | 0                              | <b>15.8</b>                    |
|              |          |                              | A       | 20–30      | 7.3     | 469       | 275                                       | n.a.  | 0.7                            | 12.2                           |
|              | SPAV13-B | Coniferous trees             | OF      | 5–7        | 27.9    | 376       | 408                                       | 242   | 20.4                           | 26.7                           |
|              |          |                              | OH      | 7–9        | 14.5    | 464       | 327                                       | 256   | 5.6                            | 30.9                           |
|              |          |                              | A       | 10–30      | 10.3    | 474       | 251                                       | 210   | 1.0                            | 20.7                           |
|              |          |                              | A       | 30–50      | 11.5    | 476       | 256                                       | 227   | 0.8                            | 21.3                           |
|              |          |                              | C       | 50–80      | 2.2     | 472       | 150                                       | 321   | n.a.                           | n.a.                           |
| CHAUVET      | SCHA15-A | Deciduous trees              | OH      | 0–15       | 23.5    | 467       | 310                                       | 170   | 10.7                           | 31.0                           |
|              |          |                              | A       | 15–30      | 14.4    | 465       | 308                                       | 188   | 8.5                            | <b>22.5</b>                    |
|              |          |                              | A       | 30–50      | 10.8    | 471       | 247                                       | 233   | 1.6                            | 15.9                           |
|              | SCHA15-B | Grassland                    | A       | 0–10       | 8.8     | 473       | 213                                       | 208   | 6.6                            | <b>16.5</b>                    |
|              |          |                              | A       | 10–40      | 7.7     | 473       | 192                                       | 231   | 0.4                            | 2.1                            |
|              |          |                              | A       | 10–40      | 7.7     | 473       | 192                                       | 231   | 0.4                            | 2.1                            |
| MONT-CINEYRE | SMO13-A  | Deciduous trees              | OL      | 0–3        | 41.1    | 364       | 310                                       | 176   | n.a.                           | n.a.                           |
|              |          |                              | OF      | 3–7        | 34.9    | 368       | 323                                       | 211   | 11.1                           | 20.6                           |
|              |          |                              | OH      | 7–15       | 21.4    | 433       | 522                                       | 278   | 16.5                           | 32.6                           |
|              |          |                              | A       | 15–30      | 14.2    | 468       | 343                                       | 244   | 1.8                            | <b>22.0</b>                    |
|              |          |                              | A       | 30–40      | 7.7     | 473       | 280                                       | 304   | 0                              | 5.9                            |
|              |          |                              | C       | 40–60      | 2.2     | 472       | 132                                       | 394   | n.a.                           | n.a.                           |
|              | SMO13-B  | Grassland                    | A       | 0–10       | 11.2    | 472       | 333                                       | 223   | 3.3                            | <b>13.9</b>                    |
|              |          |                              | A       | 10–20      | 11.3    | 472       | 327                                       | 228   | 0.1                            | 14.0                           |
|              |          |                              | A       | 20–35      | 7.0     | 474       | 227                                       | 256   | 0.4                            | 7.4                            |
|              | SMO13-C  | Coniferous trees             | OL      | 0–2        | 42.1    | 374       | 368                                       | 166   | n.a.                           | n.a.                           |
|              |          |                              | OF      | 2–6        | 32.4    | 377       | 424                                       | 172   | 15.6                           | 17.9                           |
|              |          |                              | OH      | 6–15       | 17.0    | 463       | 423                                       | 240   | 8.9                            | 37.7                           |
| A            | 15–35    | 7.3                          | 473     | 285        | 235     | 0.6       | 11.5                                      |   |                                |                                |
| C            | 35–50    | 1.7                          | 476     | 176        | 390     | n.a.      | n.a.                                      |   |                                |                                |

n.a.: not available.

(Chassiot et al., 2018).

#### 4.2.2. Lake Chauvet

Core CHA13-7B displays three sedimentary units (U1, U2, U3) where U2 is interrupted by a 10-cm thick turbidite (Chassiot et al., 2016b) (Fig. 5A). Unit U3 is faintly laminated with mean TOC content of 11% and HI values of ca. 200 mgHC.gTOC<sup>-1</sup> of HI. QOP indicates the organic content of this unit is essentially made of rAP (Fig. 5A). The onset of unit U2 is associated with a shift in organic content underlined by a decrease in TOC from 11 to 7%, an increase of HI values from 200 to 350 mgHC.gTOC<sup>-1</sup> and prevalence of AOM. Unit U1 shares the organic signatures with U2 except an upward increase of TOC. The age-depth model indicates this core covers ca. 3000 years with low SR during U3 and U1 (0.25 mm.yr<sup>-1</sup>), while U2 is characterized by higher SR (1.80 mm.yr<sup>-1</sup>).

Hydro-acoustic data display a sediment thickness reaching 5 m in the deepest location (Fig. 5B). According to Chapron et al. (2012) and Chassiot et al. (2016b), two main acoustic facies can be depicted from

acoustic images: (1) transparent to locally chaotic facies for the upper sedimentary units, and (2) stratified facies displaying high-amplitude and continuous reflections in the deep sub-basins. The calculation of SY over the 3000-year record was performed using two different sedimentation surfaces (Fig. 5B). Seismic-to-core correlation shows that the upper units U1 and U2 can be extrapolated to the surface located below 10 m water depth, where a lacustrine drape is identified on hydro-acoustic images (Chassiot et al., 2016b). This surface corresponds to a 'flat' area of 410,000 m<sup>2</sup> not considering the semi-ellipsoidal shape typical of a maar lake. Consequently, a 'corrected' sedimentation surface has been calculated using equations from Degeai and Pastre (2009) applied to the nearby maar Lake Bouchet (Fig. 1A). This correction allows us to estimate the sedimentation surface for U1 and U2 to 440,000 m<sup>2</sup>. Seismic-to-core correlation for unit U3 is less obvious on hydro-acoustic images, but this unit was not identified in other cores collected in shallower parts of the lake (Juvigné, 1992; Chapron et al., 2016). Its extent is limited to the surface below 50 m water depth, where

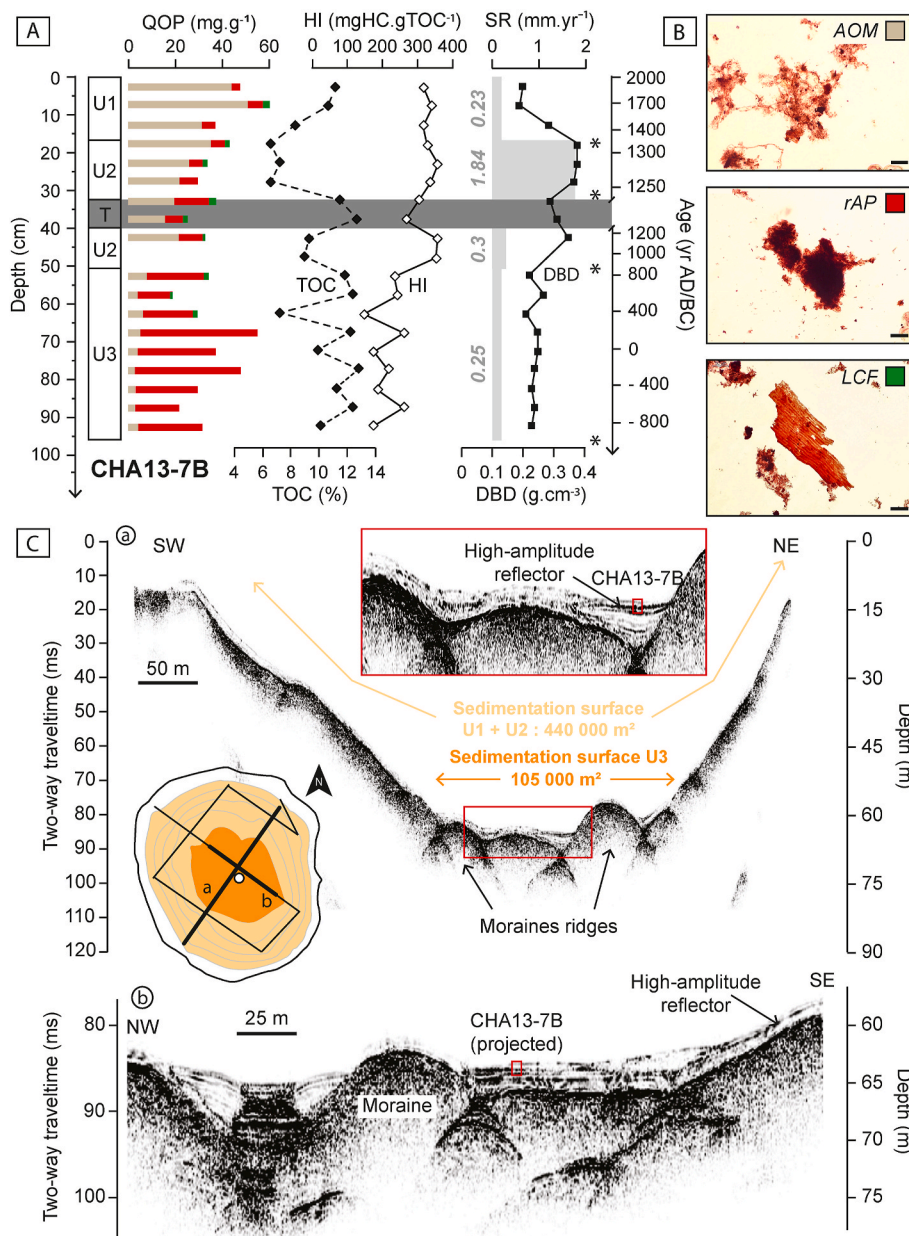


**Fig. 5.** (A) Organic signatures and chronological framework for core CHA13-7B from Lake Chauvet (French Massif Central). Asterisks indicate age controls. QOP: Quantitative Organic Petrography. TOC: Total Organic Carbon, HI: Hydrogen Index, DBD: Dry Bulk Density, SR: Sedimentation Rate. (B) Photographs displaying organic compounds. AOM: Amorphous Organic Matter (primary production), rAP: red Amorphous Particles (soils), LCF: Ligno-cellulosic Fragments (upland vegetation). Black bars correspond to 50 μm. (C) Hydro-acoustic images across Lake Chauvet. Map of sedimentation surfaces with core (white dot) and seismic survey (black line) location. (For interpretation of the references to colour in this figure legend, the reader is referred to the Web version of this article.)



the bottom of the lake is characterized by an irregular morphology made of small basins with moraine ridges. Here, the acoustic facies is stratified and characterized by high-amplitude reflections at the core location. Laterally, chaotic facies associated to reworked deposits are also identified (Fig. 5B). Using the 50 m isobath, the sedimentation surface of unit U3 can be estimated to 105,000 m<sup>2</sup>.

#### 4.2.3. Lake Montcineyre

Core MO10-H, collected on the gentle slopes of the northern basin, displays a succession of massive and organic-rich units (U1, U2, U3) (Chapron et al., 2012; Chassiot et al., 2016b) (Fig. 6A). These units represent background sedimentation with DBD ranging from 0.30 to 0.44 g cm<sup>-3</sup>. The maximal values of HI and TOC content are reached in U3 at the bottom of the core where QOP indicates an elevated proportion of in-situ organic matter (AOM). Unit U2 displays TOC values between 7 and 10% along with almost constant HI values around 350–400

mgHC.gTOC<sup>-1</sup>. Unit U1 displays a TOC content above 10%, HI values around 400 mgHC.gTOC<sup>-1</sup>, and a higher proportion of in-situ organic matter (AOM). The age-depth model indicates this core covers the past 700 years with a drastic decrease in SR from 4.44 to 0.28 mm.yr<sup>-1</sup> at the transition between U2 and U1 (Chassiot et al., 2016b).

Hydro-acoustic surveys attest of a nearly homogenous sedimentation developing a lacustrine drape geometry characterized by a continuous high amplitude reflector (labelled R1) across the lake and a maximum sediment thickness of 4 m in the deepest parts of the lake (Chapron et al., 2012; Chassiot et al., 2016b) (Fig. 6B). Seismic-to-core correlation indicates the transition between U3 and U2 at 66 cm depth matches the reflector R1. The calculation of SY over the last 700 years has thus been made considering a sedimentation surface of 190,000 m<sup>2</sup> based on the mapping of this reflector (Chassiot et al., 2016b) across the two sub-basins (Fig. 6B).

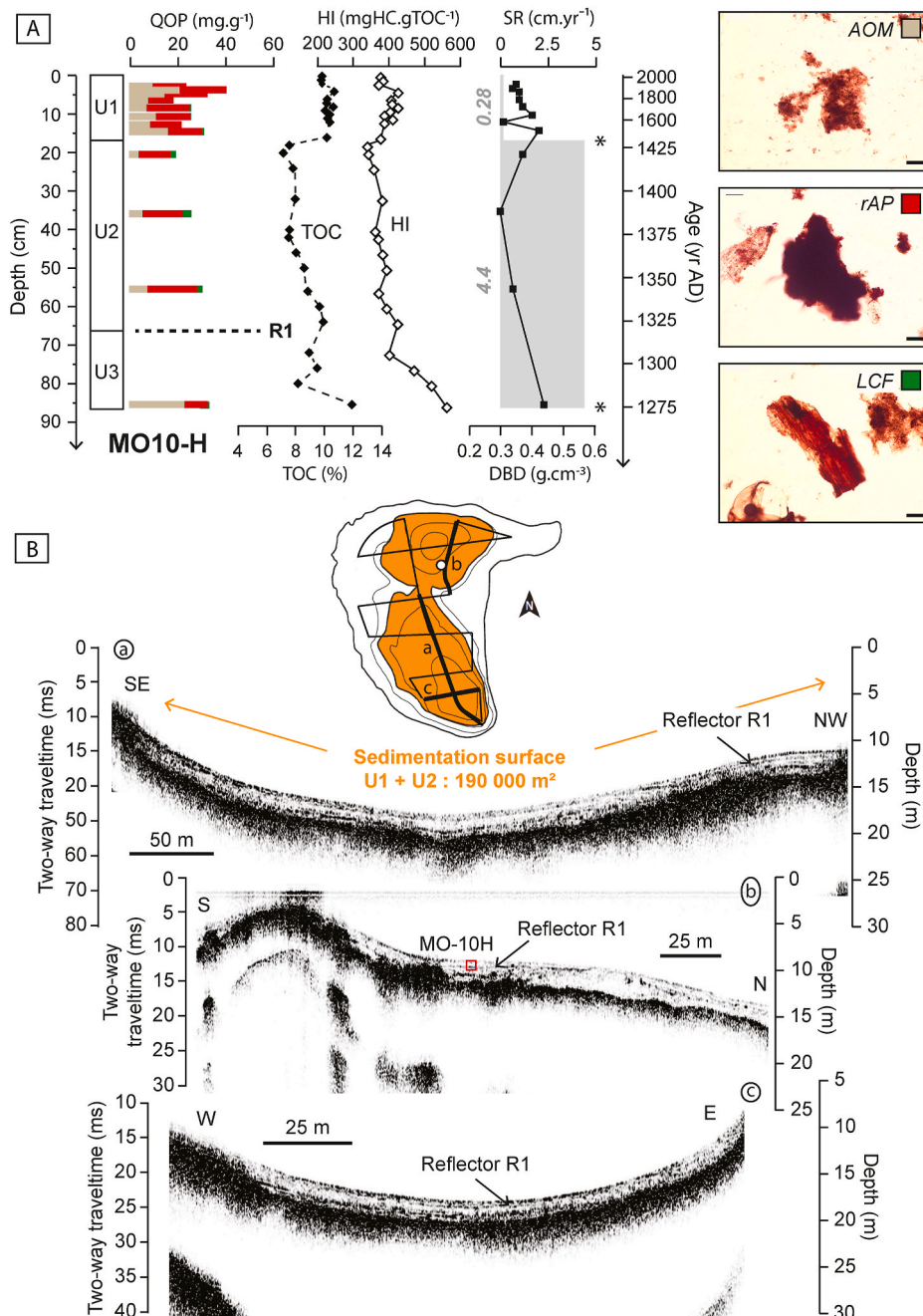


**Fig. 6.** (A) Organic signatures and chronological framework for core MO10-H from Lake Montcineyre (French Massif Central). Asterisks indicate age controls. QOP: Quantitative Organic Petrography. TOC: Total Organic Carbon, HI: Hydrogen Index, DBD: Dry Bulk Density, SR: Sedimentation Rate. (B) Photographs displaying organic compounds. AOM: Amorphous Organic Matter (primary production), rAP: red Amorphous Particles (soils), LCF: Lignocellulosic Fragments (upland vegetation). Black bars correspond to 50  $\mu$ m. (C) 12 kHz hydro-acoustic images across Lake Montcineyre. Map of sedimentation surface (orange area) with core (white dot) and seismic surveys (black line). (For interpretation of the references to colour in this figure legend, the reader is referred to the Web version of this article.)

4.3. Sediment yield records in the French Massif Central

Historical SY estimations for the Lakes Pavin, Chauvet and Montcineyre are displayed on Fig. 7B, respectively. SY vary between 3 and 320 t km<sup>-2</sup>.yr<sup>-1</sup> throughout the records over the last 700 years. Lake Pavin records values rising from 15 to 50 t km<sup>-2</sup>.yr<sup>-1</sup> between 1300 CE and 1500. After this date, SY oscillated between 50 and 196 t km<sup>-2</sup>.yr<sup>-1</sup> and reached a maximum of 196 t km<sup>-2</sup>.yr<sup>-1</sup> in ca. 1630 CE while the modern SY is around 25 t km<sup>-2</sup>.yr<sup>-1</sup>. Lakes Chauvet and Montcineyre synchronously record a drastic drop in SY at the early XV<sup>th</sup> century (i.e., ca. 1450 CE). However, values greatly differ between both sites, ranging between 3 and 90 t km<sup>-2</sup>.yr<sup>-1</sup> for Chauvet and between 10 and 320 t km<sup>-2</sup>.yr<sup>-1</sup> for Montcineyre (mean of 72 t km<sup>-2</sup>.yr<sup>-1</sup>). Maximal values in both records match the deposition of units U2 corresponding to the time intervals 850–1400 CE in Lake Chauvet and 1275–1450 CE in Lake Montcineyre, respectively. Both records finally show slight fluctuations between 3 and 20 t km<sup>-2</sup>.yr<sup>-1</sup> during the deposition of units U1 during the last 500–600 years, which is ten to fifteen times lower compared to SY during the units U2.

5. Discussion

5.1. Comparison with other lacustrine records of sediment yield

The range of historical SY values, between 3 and 320 t km<sup>-2</sup>.yr<sup>-1</sup>, is close to other lake-based SY reconstructions performed in similar morphological, geological and climatic settings. In the FMC, Gay and Macaire (1999) estimated SY between 100 and 300 t km<sup>-2</sup>.yr<sup>-1</sup> for the past 2500 years at nearby Lake Chambon (Fig. 1). There, elevated SY values were a consequence of intense erosion over a large and steep catchment drained by a river with a torrential regime. Conversely, SY reconstructions based on maar lake sediments at Lake Bouchet (Degeai and Pastre, 2009) (Fig. 1) and at Lake Holzmaar (Zolitschka, 1998) in the Eifel volcanic province (Germany) displayed lower values, between 15 and 50 t km<sup>-2</sup>.yr<sup>-1</sup> over the past 3000 years, close to SY estimates obtained at the lakes Chauvet and Pavin.

5.2. Modern sediment yield versus predicted soil erosion rates

SY represents the amount of sediments delivered by the catchment to the lake (e.g., Walling, 1983; de Vente and Poesen, 2005; de Vente et al., 2007). The spatial distribution of predicted soil erosion rates (SER) from RUSLE2015, a model of soil erosion mapped at European scale in a 100

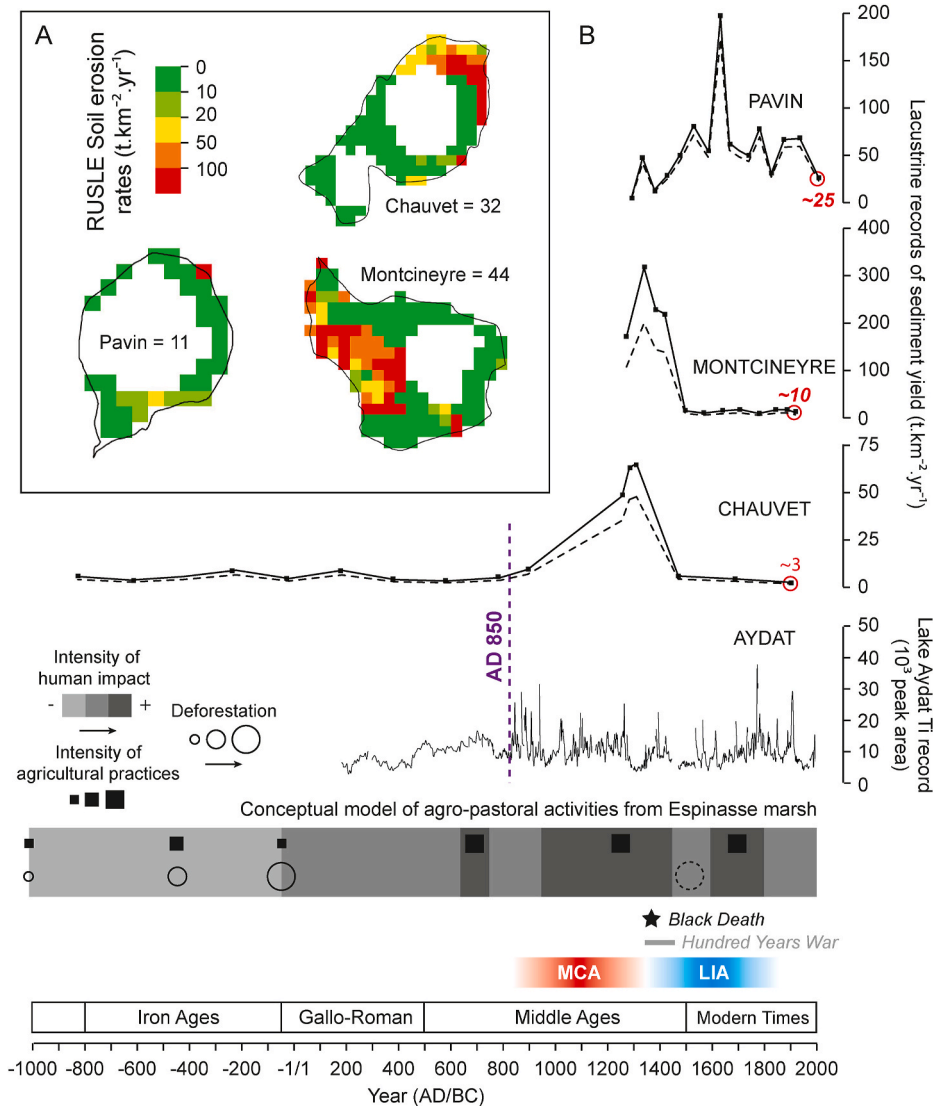


Fig. 7. (A) Predicted soil erosion rates with averaged data for each catchment (P: Pavin, C: Chauvet, M: Montcineyre; reference year: 2010). Data extracted from the map of soil loss rates in the European Union (grid of 100 × 100 m) are based on RUSLE2015 (Panagos et al., 2015) (source: <http://esdac.jrc.ec.europa.eu>). (B) Sediment yield reconstructions for lakes Pavin, Chauvet and Montcineyre using soils from grasslands (solid line) or deciduous forests (dashed line) along with the Ti record from Lake Aydat (Lavrieux et al., 2013a), major historical events, and a conceptual model of agro-pastoral activities derived from the multi-proxy study of the Espinasse marsh (Miras et al., 2004), and climatic phases of the last millennium: Medieval Climate Anomaly (MCA) and Little Ice Age (LIA). (For interpretation of the references to colour in this figure legend, the reader is referred to the Web version of this article.)

m × 100 m grid (Panagos et al., 2015), shows highest values for grassland areas (Figs. 1B and 7A), meaning land cover is the primary driver controlling erosion in the studied catchments. Modern values of SY for Chauvet, Montcineyre and Pavin are equal to 3, 10 and 25 t km<sup>-2</sup>.yr<sup>-1</sup> (Fig. 7B), respectively, whereas averaged SER values at catchment scale are 32, 44, and 11 t km<sup>-2</sup>.yr<sup>-1</sup>, respectively (Fig. 7A). At Pavin, comparison between both datasets indicates estimated SY values that are twice as high than predicted SER values, suggesting SY includes a significant part of geomorphic processes such as snowmelt, rain-on-snow events, gully erosion (not accounted in the RUSLE2015 model) and/or scale issues between predicted SER and catchment SY (e.g., de Vente and Poesen, 2005; Vanmaercke et al., 2012). At Chauvet and Montcineyre, comparison between both datasets indicates a sediment delivery ratio (i.e., the ratio between sediment yield and soil erosion; e.g., Walling, 1983; de Vente et al., 2007) of 10% and 23%, respectively. These findings suggest either a storage of eroded material within catchments or sediment export through the outlet. This latter hypothesis is excluded since none or limited outflows currently exist and their high aspect ratios make them efficient traps for sediments (Table 1). Although their small catchment size (<1 km<sup>2</sup>, Table 1) should also limit the transport duration between sources and sink as well as storage within the catchment (Dearing and Jones, 2003), the low delivery ratios identified at Chauvet and Montcineyre could be a consequence of peatlands acting as up-stream sediment traps (Fig. 2).

### 5.3. Natural versus anthropogenic signals on sediment yield records

Over the past 700 years, mean values of SY were elevated at Lake Pavin (50 t km<sup>-2</sup>.yr<sup>-1</sup>, Fig. 7B), which may be related to the steep morphology of its catchment (Table 1, Fig. 1) and the fragile nature of soils developed over pumice and trachy-basaltic lavas (Bourdier, 1980) developing gullies, soils ripple, creep and small landslides (Thouret et al., 2016). However, the modern values are lower, around 25 t km<sup>-2</sup>.yr<sup>-1</sup> (Fig. 7B), likely as a result of (1) afforestation in the catchment reducing sediment transfer to the lake (Stebich et al., 2005); (2) reduced precipitation following the end of the Little Ice Age (LIA) in Western Europe (Mann et al., 2009). The pollen analysis at Lake Pavin showed a predominance of forests with a patchwork of open areas for the past 700 years (Stebich et al., 2005; Chassiot et al., 2018), suggesting forest clearance within the catchment. Regular occurrences of spores of *coprophilous fungi* also document grazing activity, suggesting humans and their livestock may have influenced erosion processes in the catchment during this period (Chassiot et al., 2018). However, the influence of human activities in the past 700 years shall not overlook the role of climate during the LIA (Chassiot et al., 2018).

Historical SY values recorded in Montcineyre (mean of 193 t km<sup>-2</sup>.yr<sup>-1</sup> during Medieval Times (unit U2) and 12 t km<sup>-2</sup>.yr<sup>-1</sup> thereafter (unit U1), Fig. 7B) were higher than in Chauvet (mean of 54 t km<sup>-2</sup>.yr<sup>-1</sup> during Medieval Times (unit U2) and 5 t km<sup>-2</sup>.yr<sup>-1</sup> thereafter (unit U1), Fig. 7B). This difference may be a consequence of (1) the presence of a peatland upstream the river flowing in the catchment of Chauvet, and thus lowering sediment export to the lake (Figs. 1 and 2); (2) a steeper catchment for Lake Montcineyre, with a slope >45° in the eastern part (Table 1, Fig. 2); and (3) the Montcineyre soil lithology, developed on ca. 7000-yr old volcanic products, i.e., pumices from Pavin and scoria from Montcineyre (Bourdier, 1980; Juvigné et al., 1996), which is more recent and prone to erosion than soils developed on basaltic and plutonic rocks identified within the catchment of Chauvet (Brousse et al., 1990).

Historical SY values recorded at lakes Chauvet and Montcineyre are nearly constant over the past 500 years, ranging from 3 to 15 t km<sup>-2</sup>.yr<sup>-1</sup>. This stable situation underlines either the absence of environmental changes during this period, or slight modifications in land use and/or vegetation cover that did not significantly affect SY. Formerly, both sites synchronously recorded their highest SY values between 850 CE and 1450 CE, which suggest a common factor having driven erosional processes. This period corresponds to the Medieval Climate Anomaly (MCA),

characterized by higher-than-normal temperatures in the northern hemisphere (Mann et al., 2009). Tree-ring reconstructions indicate fluctuating but slightly higher-than-normal precipitation patterns for Western-Central Europe (Büntgen et al., 2011) during that time, but the Alpine stacked record of lake-levels indicate no high stands between 850 CE and 1200 CE (Magny, 2004). Therefore, it seems unlikely that the shift (a ten to fifteen times decrease) observed in historical SY was related to precipitation changes over the FMC. Alternatively, land use change could be the origin of this shift. Human occupation in this area is furthermore supported by (1) half-buried pastoral structures reported from the catchments (Fig. 1C); (2) faecal biomarkers of cows identified in the sedimentary record of Lake Montcineyre (Zocatelli et al., 2017); and (3) landscape opening with an onset of agriculture after the mid-VII<sup>th</sup> century as reported from nearby pollen record collected at Lake Chambedaze (Fig. 1B) (Guenet and Reille, 1988). Therefore, intense soil erosion in response to agricultural activities that have prevailed between 850 CE and 1400 CE in Lake Chauvet and from 1275 CE to 1450 CE in Lake Montcineyre. The occurrence of faecal biomarkers throughout the record of Lake Montcineyre indicates pastoral activities have also occurred with a peak in livestock population between 1300 CE and 1400 CE (Zocatelli et al., 2017). Recent archaeological investigations south of Montcineyre also revealed numerous medieval dwellings occupied during the XI<sup>th</sup> and XII<sup>th</sup> century (Surmely, personal communication), in agreement with a rural demography once spread in mid-altitude hamlets (Fournier, 1962). However, to date, the link between historical land use, soil erosion and archaeological structures (Fig. 1) remains uncertain.

The onset of unit U2 dated at 850 CE in core CHA13-7B from Lake Chauvet is underlined by drastic geochemical and sedimentary shifts (Fig. 5A, Chassiot et al., 2016b). At Lake Aydat (Fig. 1A), this date corresponds to the beginning of hemp retting, which is accompanied by a doubling in sedimentation rates, an increase of terrigenous signal (Ti record in Fig. 7B) and a sedimentation shift with the occurrence of flood layers (Lavrieux et al., 2013a, 2013b). According to the conceptual model of agro-pastoral activities based on a multi-proxy study of the Espinasse peat marsh (Miras et al., 2004) (Figs. 1A and 7B), a generalized practice of agriculture is documented from the Early Middle Ages until the late XIX<sup>th</sup> century. Agro-pastoral activities in the region were accompanied with a significant deforestation, with forest cover falling to 15–45% at the regional level (Miras et al., 2018). The importance of agriculture over the same period was later confirmed by the multi-proxy study of the Lake Aydat sediment record (Lavrieux et al., 2013a, 2013b). This is not the case for Chauvet and Montcineyre, where a drastic shift in land use occurred at the early XV<sup>th</sup> century. At this time, a slight decline of anthropogenic pressure was reported in the Espinasse peat marsh (Miras et al., 2004). At Chauvet and Montcineyre, historical causes driving this shift remain unclear as historical archives and archaeological investigations are lacking. Here, the land-use shift could result either from a demographic decline, or from a socio-economic evolution leading to a replacement of arable lands by pastures. Although fiefdom instabilities are documented across the FMC during the XIV<sup>th</sup> and XV<sup>th</sup> centuries (Charbonnier, 1999), a demographic decline is not attested in this remote area. The drastic drop in SY may be an indirect consequence of two dramatic events: the Black Death in 1348–1352 CE and the Hundred Years War between 1337 and 1453 CE. Palaeoecological modelling suggested the French Massif Central was severely affected by the Black Death (Izdebski et al., 2021). About the Hundred Years War, only a royal letter mentions troubles in the area of Montcineyre (Chassaing, 1886; Boyer-Gouédard, personal communication; source: <http://www.compains-cezallier.com>). Did these events really affect the demographics and livelihoods around Montcineyre at that time? Historical research would help clarify this point.

Despite the importance of human activities in the area, variations in SY may also have been directly, or indirectly influenced by climatic variations. As an example, the almost synchronous record of high SY in 1320 CE between the three sites may be a result of a regional climatic deterioration (Fig. 7B). Still, the pattern of historical SY at Chauvet and

Montcineyre, with the lowest values recorded during the LIA, supports the conclusions of [Paroissien et al. \(2015\)](#) suggesting soil erosion rates are more sensitive to land use changes rather than precipitation changes expected from climatic projections. Climate may, however, influence human societies by promoting new agricultural practices. Indeed, the land use shift promoting pastoral activities could be a local adaptation to the coldest decades documented across Europe around 1430 CE ([Camenisch, 2015](#); [Camenisch et al., 2016](#)). In conclusion, the sedimentary records from Chauvet and Montcineyre suggest that the decline of the SY in the early XV<sup>th</sup> century resulted from a major change in agropastoral practices in the region, probably related to historical events of the previous century and/or unstable climatic conditions.

## 6. Conclusions

The use of rAP as a tracer of historical SY in lacustrine records has been successfully achieved within three contrasted lake-catchment systems including two maar lakes (Pavin and Chauvet) and one volcano-dammed lake (Montcineyre). For the past millennium, SY values range between 3 and 320 t km<sup>-2</sup>.yr<sup>-1</sup>. Elevated mean slope values characterize catchments with the highest mean SY (Pavin and Montcineyre). Climate variability during the LIA and human activities such as woodland clearance and grazing activities both influenced historical SY recorded at Pavin. Few kilometres south, significant geochemical and sedimentary changes were recorded in the Lakes Chauvet and Montcineyre. Historical SY, accompanied by major shifts in organic content and organic matter composition attest for a common factor having affected the catchments and lake dynamics. Both records displayed maximum values during the Middle Ages (850–1450 CE), likely associated with the expansion of agricultural practices, in agreement with previous studies from Lake Aydat and Espinasse peat marsh records. Later, a major event occurred in the early XV<sup>th</sup> century with a ten to fifteen-fold decrease in sediment yields resulting from a change in agro-pastoral practices. Historical archives suggest that this change may be consecutive to a drop in rural population density, political turmoil during this period, and/or cultural adaptation to a colder climate during the LIA. Additional investigations on Holocene sedimentary records, historical documents and archaeological sites are needed to complement this study and document the dynamics of human settlement in rural areas of the French Massif Central. More generally, this work highlights the relevance of lake sediment erosion records to document long-term ecological trajectories and to assess relationships between climate change, human societies, vegetation cover, land use and erosion processes at catchment scale. Such studies are required for the FMC where human-climate-environment interactions during the Holocene remains poorly understood.

## Declaration of competing interest

The authors declare that they have no known competing financial interests or personal relationships that could have appeared to influence the work reported in this paper.

## Acknowledgements

This manuscript is dedicated to the memory of Pr. Christian Di Giovanni, a professor and colleague very much appreciated by his peers, for his involvement in the laboratory and with the students in Earth Sciences at the University of Orléans. We warmly greet his implication in the ISTO laboratory on lake archives and organic matter, and in particular his investment in the training of young scientists at the University of Orléans. Many of us owe our academic success to him. This study is part of Léo Chassiot's PhD at the University of Orléans funded by a grant from the Région Centre Val-de-Loire and the EDIFIS project (2012–2016) from the Loire-Brittany Water Agency. Authors thank Patrick Lajeunesse, Guillaume St-Onge, Grégoire Ledoux and MSc

students from the University of Orléans for active participation in hydro-acoustic surveys and coring operations. Fruitful discussions with Yannick Miras and Frédéric Surmely greatly helped to design this manuscript. The meticulous work of Anne-Marie Boyer-Gouédard provided important insights about the regional history around Lake Montcineyre, and is also gratefully acknowledged. This manuscript finally benefitted from constructive remarks of two anonymous reviewers and corrections from the guest editor Jean Nicolas Haas.

## References

- Allen, D., Simonneau, A., Le Roux, G., Mazier, F., Marquer, L., Galop, D., 2020. Considering lacustrine erosion records and the De Ploey erosion model in an examination of mountain catchment erosion susceptibility and total rainfall reconstruction. *Catena* 187, 104278.
- Anselmetti, F.S., Hodel, D.A., Ariztegui, D., Brenner, M., Rosenmeier, M.F., 2007. Quantification of soil erosion rates related to ancient Maya deforestation. *Geology* 35, 915–918.
- Arnaud, F., Poulenard, J., Giguet-Covex, C., Wilhelm, B., Révillon, S., Jenny, J.-P., Revel, M., Enters, D., Bajard, M., Fouinat, L., Doyen, E., Simonneau, A., Pignol, C., Chapron, E., Vannière, B., Sabatier, P., 2016. Erosion under climate and human pressures: an alpine lake sediment perspective. *Quat. Sci. Rev.* 152, 1–18.
- Bajard, M., Poulenard, J., Sabatier, P., Develle, A.-L., Giguet-Covex, C., Jacob, J., Crouzet, C., David, F., Pignol, C., Arnaud, F., 2017. Progressive and regressive soil evolution phases in the Anthropocene. *Catena* 150, 39–52. <https://doi.org/10.1016/j.catena.2016.11.001>.
- Barreiro-Lostres, F., Moreno, A., González-Sampérez, P., Giralt, S., Nadal-Romero, E., Valero-Garcés, B., 2017. Erosion in Mediterranean mountain landscapes during the last millennium: a quantitative approach based on lake sediment sequences (Iberian Range, Spain). *Catena* 149, 782–798. <https://doi.org/10.1016/j.catena.2016.05.024>.
- Behar, F., Beaumont, V., Penteado, H.D.B., 2001. Rock-Eval 6 technology: performances and developments. *Oil Gas Sci. Technol.* 56, 111–134.
- Bourdier, J.-L., 1980. Contribution à l'étude volcanologique de deux secteurs d'intérêt géothermique dans le Mont Dore: le groupe holocène du Pavin et le Massif du Sancy. Thèse de l'Université d'Orléans, p. 180.
- Breuer, S., Kilian, R., Baeza, O., Lamy, F., Arz, H., 2013. Holocene denudation rates from the superhumid southernmost Chilean Patagonian Andes (53°S) deduced from lake sediment budgets. *Geomorphology* 187, 135–152. <https://doi.org/10.1016/j.geomorph.2013.01.009>.
- Brisset, E., Guitier, F., Miramont, C., Troussier, T., Sabatier, P., Poher, Y., Cartier, R., Arnaud, F., Malet, E., Anthony, E.J., 2017. The overlooked human influence in historic and prehistoric floods in the European Alps. *Geology* 45, 347–350.
- Brousse, P., Rançon, J.-P., Le Garrec, M.-J., Tempier, P., Suire, J., Veyret-Mekdjian, Y., D'Arcy, D., Perichaud, J.-J., 1990. Notice explicative, carte géologique de France (1/50000), feuille La Tour-d'Auvergne (740), Orléans. Bureau de Recherches Géologiques et Minières, p. 68.
- Büntgen, U., Tegel, W., Nicolussi, K., McCormick, M., Frank, D., Trouet, V., Kaplan, J.O., Herzog, F., Heussner, K.U., Wanner, H., Luterbacher, J., Esper, J., 2011. 2500 years of European climate variability and human susceptibility. *Science* 331, 578–582.
- Camenisch, 2015. Endless cold: a seasonal reconstruction of temperature and precipitation in the Burgundian Low Countries during the 15th century based on documentary evidence. *Clim. Past* 11, 1049–1066.
- Camenisch, C., Keller, K.M., Salvisberg, M., Amann, B., Bauch, M., Blumer, S., Brázdil, R., Brönnimann, S., Büntgen, U., Campbell, B.M.S., Fernández-Donado, L., Fleitmann, D., Glaser, R., González-Rouco, F., Grosjean, M., Hoffmann, R.C., Huhtamaa, H., Joos, F., Kiss, A., Kotyza, O., Lehner, F., Luterbacher, J., Maughan, N., Neukom, R., Novy, T., Pribyl, K., Raible, C.C., Riemann, D., Schuh, M., Slavin, P., Werner, J.P., Wetter, O., 2016. The 1430s: a cold period of extraordinary internal climate variability during the early Spörer Minimum with social and economic impacts in north-western and central Europe. *Clim. Past* 12, 2107–2126. <https://doi.org/10.5194/cp-12-2107-2016>.
- Chapron, E., Albéric, P., Jézéquel, D., Versteeg, W., Bourdier, J.-L., Sitbon, J., 2010. Multidisciplinary characterisation of sedimentary processes in a recent maar lake (Lake Pavin, French Massif Central) and implication for natural hazards. *Nat. Hazards Earth Syst. Sci.* 10, 1815–1827. <https://doi.org/10.5194/nhess-10-1815-2010>.
- Chapron, E., Chassiot, L., Lajeunesse, P., Ledoux, G., Albéric, P., 2016. Lake Pavin sedimentary environments. In: Sime-Ngando, T., Boivin, P., Chapron, E., Jézéquel, D., Meybeck, M. (Eds.), *Lake Pavin: History, Geology, Biogeochemistry and Sedimentology of a Deep Meromictic Maar Lake*. Springer Switzerland, Cham, pp. 365–379.
- Chapron, E., Ledoux, G., Simonneau, A., Albéric, P., St-Onge, G., Lajeunesse, P., Boivin, P., Desmet, M., 2012. New evidence of Holocene mass wasting events in recent volcanic lakes from the French Massif central (lakes Pavin, Montcineyre and Chauvet) and implications for natural hazards. In: Yamada, Y., Kawamura, K., Ikehara, K., Ogawa, Y., Urgeles, R., Mosher, D., Chaytor, J., Strasser, M. (Eds.), *Submarine Mass Movements and Their Consequences*. Springer Netherlands, Dordrecht, pp. 255–264.
- Charbonnier, P., 1999. Histoire de l'Auvergne des origines à nos jours. Haute et Basse-Auvergne. Bourbonnais et Velay, p. 540.
- Chassaing, A., 1886. *Spicilegium Brivatense. Recueil de documents historiques relatifs à l'Auvergne et au Brivadois*. Imprimerie Nationale de Paris, p. 796.

- Chassiot, L., Chapron, E., Di Giovanni, C., Albéric, P., Lajeunesse, P., Lehours, A.-C., Meybeck, M., 2016a. Extreme events in the sedimentary record of maar Lake Pavin: implications for natural hazards assessment in the French Massif Central. *Quat. Sci. Rev.* 141, 9–25. <https://doi.org/10.1016/j.quascirev.2016.03.020>.
- Chassiot, L., Chapron, E., Di Giovanni, C., Lajeunesse, P., Tachikawa, K., Garcia, M., Bard, E., 2016b. Historical seismicity of the Mont Dore volcanic province (Auvergne, France) unraveled by a regional lacustrine investigation: new insights about lake sensitivity to earthquakes. *Sediment. Geol.* 339, 134–150. <https://doi.org/10.1016/j.sedgeo.2016.04.007>.
- Chassiot, L., Chapron, E., Miras, M., Develle, A.-L., Arnaud, F., Motelica-Heino, M., Di Giovanni, C., 2018. A 7,000-year environmental history and soil erosion record inferred from the deep sediments of Lake Pavin (Massif Central, France). *Palaeogeogr. Palaeoclimatol. Palaeoecol.* 497, 218–233.
- Combaz, A., 1964. Les palynofaciès. *Rev. Micropaleontol.* 7, 205–218.
- Daugas, J.-P., Raynal, J.-P., 1989. Quelques étapes du peuplement du Massif Central français dans leur contexte paléoclimatique et paléogéographique. In: Laville, H. (Ed.), *Variations des Paléomilieus et Peuplement Préhistorique. Colloque du Comité Français de l'Union Internationale pour l'étude du Quaternaire (INQUA). Cahiers du Quaternaire*, vol. 13. CNRS Editions, pp. 67–95.
- de Vente, J., Poesen, J., 2005. Predicting soil erosion and sediment yield at the basin scale: scale issues and semi-quantitative models. *Earth Sci. Rev.* 71, 95–125.
- de Vente, J., Poesen, J., Arabkhedri, M., Verstraeten, G., 2007. The sediment delivery problem revisited. *Prog. Phys. Geogr.* 31, 155–178.
- Dearing, J.A., Battarbee, R.W., Dikau, R., Larocque, I., Oldfield, F., 2006. Human–environment interactions: learning from the past. *Reg. Environ. Change* 6, 1–16. <https://doi.org/10.1007/s10113-005-0011-8>.
- Dearing, J.A., Braimoh, A.K., Reenberg, A., Turner, B.L., van der Leeuw, S., 2010. Complex land systems: the need for long time perspectives to assess their future. *Ecol. Soc.* 15, 21.
- Dearing, J.A., Håkansson, H., Liedberg-Jönsson, B., Persson, A., Skansjö, S., Widholm, D., El-Daoushy, F., 1987. Lake Sediments used to quantify the erosional response to land use change in Southern Sweden. *Oikos* 50, 60–78. <https://doi.org/10.2307/3565402>.
- Dearing, J.A., Jones, R.T., 2003. Coupling temporal and spatial dimensions of global sediment flux through lake and marine sediment records. *Global Planet. Change* 39, 147–168. [https://doi.org/10.1016/S0921-8181\(03\)00022-5](https://doi.org/10.1016/S0921-8181(03)00022-5).
- Degeai, J.-P., Pastre, J.-F., 2009. Impacts environnementaux sur l'érosion des sols au Pléistocène supérieur et à l'Holocène dans le cratère de maar du lac du Bouchet (Massif central, France). *Quaternaire* 20, 149–159. <https://doi.org/10.4000/quaternaire.5101>.
- Desloges, J., 1994. Varve deposition and the sediment yield record at three small lakes of the southern Canadian Cordillera. *Arct. Alp. Res.* 50, 130–140. <https://doi.org/10.2307/1551776>.
- Di Giovanni, C., Disnar, J.-R., Bichet, V., Campy, M., Guillet, B., 1998. Geochemical characterization of soil organic matter and variability of a postglacial detrital organic supply (Chaillexon Lake, France). *Earth Surf. Process. Landforms* 23, 1057–1069.
- Disnar, J.-R., Guillet, B., Kéravis, D., Di-Giovanni, C., Sebag, D., 2003. Soil organic matter (SOM) characterization by Rock-Eval pyrolysis: scope and limitations. *Org. Geochem.* 34, 327–343.
- Einsle, G., Hinderer, M., 1998. Quantifying denudation and sediment-accumulation systems (open and closed lakes): basic concepts and first results. *Palaeogeogr. Palaeoclimatol. Palaeoecol.* 140, 7–21.
- Enters, D., Dörfler, W., Zolitschka, B., 2008. Historical soil erosion and land-use change during the last two millennia recorded in lake sediments of Frickenhauser See, northern Bavaria, central Germany. *The Holocene* 18, 243–254. <https://doi.org/10.1177/0959683607086762>.
- European Commission, 2006. Proposal for a Directive of the European Parliament and of the Council Establishing a Framework for the Soil Protection and Amending Directive 2004/35/EC. COM (2006)232 Brussels, 22/09/2006.
- Evans, M., 1997. Temporal and spatial representativeness of alpine sediment yields: Cascade Mountains, British Columbia. *Earth Surf. Process. Landforms* 22, 287–295.
- Evans, M., Church, M., 2000. A method for error analysis of sediment yields derived from estimates of lacustrine sediment accumulation. *Earth Surf. Process. Landforms* 25, 1257–1267.
- Fel, A., 1984. Histoire d'un paysage pastoral: le Massif Central. *Rev. Géogr. Alp.* 72, 253–264. <https://doi.org/10.3406/rga.1984.2568>.
- Foucher, A., Salvador-Blanes, S., Evrard, O., Simonneau, A., Chapron, E., Courp, T., Cerdan, O., Lefèvre, I., Adriaenssen, H., Lecompte, F., Desmet, M., 2014. Increase in soil erosion after agricultural intensification: evidence from a lowland basin in France. *Anthropocene* 7, 30–41. <https://doi.org/10.1016/j.anucene.2015.02.001>.
- Fournier, G., 1962. Le peuplement rural en Basse-Auvergne au Haut Moyen Age. Académie des Sciences, Belles Lettres et Arts de Clermont-Ferrand. Thèse de l'Université de Paris, Clermont-Ferrand, p. 683.
- Gaillard, M.-J., Dearing, J.A., El-Daoushy, F., Enell, M., Håkansson, H., 1991. A late Holocene record of land-use history, soil erosion, lake trophy and lake-level fluctuations at Bjäresjösjön (South Sweden). *J. Paleolimnol.* 6, 51–81.
- Garbrecht, J.D., Nearing, M.A., Douglas Shields Jr., F., Tomer, M.D., Sadler, E.J., Bonta, J.V., Baffaut, C., 2014. Impact of weather and climate scenarios on conservation assessment outcomes. *J. Soil Water Conserv.* 69, 374–392.
- Gay, I., Maccuire, J.-J., 1999. Estimation des taux d'érosion chimique tardiglaciaires et holocènes par la méthode des bilans d'altération. Application au bassin du lac Chambon (Massif Central, France). *Comptes Rendus Acad. Sci. - Ser. IIA Earth Planet. Sci.* 328, 387–392.
- Graz, Y., Di-Giovanni, C., Copard, Y., Laggoun-Défarage, F., Boussafir, M., Lallier-Vergès, E., Baillif, P., Perdereau, L., Simonneau, A., 2010. Quantitative palynofacies analysis as a new tool to study transfers of fossil organic matter in recent terrestrial environments. *Int. J. Coal Geol.* 84, 49–62. <https://doi.org/10.1016/j.coal.2010.08.006>.
- Guenet, P., Reille, M., 1988. Analyse pollinique du lac-tourbière de Chambedaze (Massif Central, France) et datation de l'explosion des plus jeunes volcans d'Auvergne. *Bull. Assoc. Fr. Étude Quat.* 25, 175–194. <https://doi.org/10.3406/quate.1988.1880>.
- Izdebski, A., Guzowski, P., Poniat, R., Masci, L., Palli, J., Vignola, C., Bauch, M., Coccozza, C., Fernandes, R., Ljungqvist, F., Newfield, T., Seim, A., Abel-Schaad, D., Alba-Sánchez, F., Björkman, L., Brauer, A., Brown, A., Czerwiński, S., Ejarque, A., Filoc, M., Florenzano, A., Fredh, E., Fyfe, R., Jasunas, N., Kolaczek, P., Kouli, K., Kozáková, R., Kupryjanowicz, M., Lagerås, P., Lamentowicz, M., Lindbladh, M., López-Sáez, J.A., Luelmo-Lautenschlaeger, R., Marcisz, K., Mazier, F., Mensing, S., Mercuri, A.M., Milecka, K., Miras, Y., Noryskiewicz, A., Nowenko, E., Obremska, M., Pędziszewska, A., Pérez-Díaz, S., Piovesan, G., Pluskowski, A., Pokorný, P., Poska, A., Reitalu, T., Rösch, M., Sadori, L., Ferreira, C.S., Sebag, D., Stowiński, M., Stancikaitė, M., Stivrins, N., Tunno, I., Veski, S., Wacnik, A., Masi, A., 2021. Big data Palaeoecology reveals significant variation in Black Death mortality in Europe (preprint). In: Review.
- Juvigné, 1992. Approche de l'âge de deux cratères volcaniques lacustres d'Auvergne (France). *Comptes Rendus de l'Académie des Sciences de Paris* 314, 401–404.
- Juvigné, E., Bastin, B., Delibrias, G., Evin, J., Gewalt, M., Gilot, E., Streeel, M., 1996. A comprehensive pollen- and tephra-based chronostratigraphic model for the Late Glacial and Holocene period in the French Massif Central. *Quat. Int.* 34, 113–120.
- Kuhlman, T., Reinhard, S., Gaaff, A., 2010. Estimating the costs and benefits of soil conservation in Europe. *Land Use Pol.* 27, 22–32. <https://doi.org/10.1016/j.landusepol.2008.08.002>.
- Lal, R., Delgado, J.A., Groffman, P.M., Millar, N., Dell, C., Rotz, A., 2011. Management to mitigate and adapt to climate change. *J. Soil Water Conserv.* 66, 276–285. <https://doi.org/10.2489/jswc.66.4.276>.
- Lamoureux, S., 2002. Temporal patterns of suspended sediment yield following moderate to extreme hydrological events recorded in varved lacustrine sediments. *Earth Surf. Process. Landforms* 27, 1107–1124. <https://doi.org/10.1002/esp.399>.
- Lavrieux, M., Disnar, J.-R., Chapron, E., Bréheret, J.-G., Jacob, J., Miras, Y., Reys, J.-L., Andrieu-Ponel, V., Arnaud, F., 2013a. 6700 yr sedimentary record of climatic and anthropogenic signals in Lake Aydat (French Massif Central). *The Holocene* 23, 1317–1328.
- Lavrieux, M., Jacob, J., Disnar, J.-R., Bréheret, J.-G., Le Milbeau, C., Miras, Y., Andrieu-Ponel, V., 2013b. Sedimentary cannabinol tracks the history of hemp retting. *Geology* 41, 751–754. <https://doi.org/10.1130/G34073.1>.
- Maccuire, J.-J., Fourmont, A., Argant, J., Bréheret, J.-G., Hinschberger, F., Trement, F., 2010. Quantitative analysis of climate versus human impact on sediment yield since the Lateglacial: the Sarliève palaeolake catchment (France). *The Holocene* 20, 497–516. <https://doi.org/10.1177/0959683609355181>.
- Magny, M., 2004. Holocene climate variability as reflected by mid-European lake-level fluctuations and its probable impact on prehistoric human settlements. *Quat. Int.* 113, 65–79.
- Mann, M.E., Zhang, Z., Rutherford, S., Bradley, R.S., Hughes, M.K., Shindell, D., Ammann, C., Faluvegi, G., Ni, F., 2009. Global signatures and dynamical origins of the Little Ice age and medieval climate anomaly. *Science* 326, 1256–1260. <https://doi.org/10.1126/science.1177303>.
- Mills, K., Schillereff, D., Saulnier-Talbot, E., Gell, P., Anderson, N.J., Arnaud, F., Dong, X., Jones, M., McGowan, S., Massafiero, J., Moorhouse, H., Perez, L., Ryves, D. B., 2017. Deciphering long-term records of natural variability and human impact as recorded in lake sediments: a palaeolimnological puzzle. *Wiley Interdisc. Rev.: Water* 4, e1195. <https://doi.org/10.1002/wat2.1195>.
- Miras, Y., Beauger, A., Lavrieux, M., Berthon, V., Serieysson, K., Andrieu-Ponel, V., Ledger, P.M., 2015. Tracking long-term human impacts on landscape, vegetal biodiversity and water quality in the Lake Aydat catchment (Auvergne, France) using pollen, non-pollen palynomorphs and diatom assemblages. *Palaeogeogr. Palaeoclimatol. Palaeoecol.* 424, 76–90. <https://doi.org/10.1016/j.palaeo.2015.02.016>.
- Miras, Y., Laggoun-Défarage, F., Guenet, P., Richard, H., 2004. Multi-disciplinary approach to changes in agro-pastoral activities since the sub-Boreal in the surroundings of the 'Narse d'Espinasse' (Puy de Dôme, French Massif central). *Veg. Hist. Archaeobotany* 13, 91–103. <https://doi.org/10.1007/s00334-004-0033-z>.
- Miras, Y., Mariani, M., Ledger, P.M., Mayoral, A., Chassiot, L., Lavrieux, M., 2018. Holocene vegetation dynamics and first land-cover estimates in the Auvergne Mountains (Massif Central, France): key tools to landscape management. *Interdiscip. Archaeol. Nat. Sci. Archaeol.* IX, 2.
- Nearing, M.A., Pruski, F., O'Neal, M.R., 2004. Expected climate change impacts on soil erosion rates: a review. *J. Soil Water Conserv.* 59, 43–50.
- O'Hara, S.L., Alayne Street-Perrott, F., Burt, T.P., 1993. Accelerated soil erosion around a Mexican highland lake caused by Hispanic agriculture. *Nature* 362, 48–51.
- Panagos, P., Borrelli, P., Poesen, J., Ballabio, C., Lugato, E., Meusburger, K., Montanarella, L., Alewell, C., 2015. The new assessment of soil loss by water erosion in Europe. *Environ. Sci. Pol.* 54, 438–447. <https://doi.org/10.1016/j.envsci.2015.08.012>.
- Paroissien, J.-B., Darboux, F., Couturier, A., Devillers, B., Mouillot, F., Raclot, D., Le Bissonnais, Y., 2015. A method for modelling the effects of climate and land use changes on erosion and sustainability of soil in a Mediterranean watershed (Languedoc, France). *J. Environ. Manag.* 150, 57–68. <https://doi.org/10.1016/j.jenvman.2014.10.034>.
- Perpère, M., 1979. Haltes préhistoriques sur les rives du Lac de Guéry (Puy-de-Dôme). *Rev. Archéol. Cent. Fr.* 18, 165–167. <https://doi.org/10.3406/racf.1979.2256>.
- Quantin, P., 2004. Volcanic soils of France. *Catena* 56, 95–109. <https://doi.org/10.1016/j.catena.2003.10.019>.

- Rioual, P., 2002. Limnological characteristics of 25 lakes of the French Massif central. *Annales de Limnologie – Int. J. Limnol.* 38, 311–327. <https://doi.org/10.1051/limn/2002026>.
- Sebag, D., Copard, Y., Di-Giovanni, C., Durand, A., Laignel, B., Ogier, S., Lallier-Verges, E., 2006a. Palynofacies as useful tool to study origins and transfers of particulate organic matter in recent terrestrial environments: synopsis and prospects. *Earth Sci. Rev.* 79, 241–259.
- Sebag, D., Disnar, J.R., Guillet, B., Di Giovanni, C., Verrecchia, E.P., Durand, A., 2006b. Monitoring organic matter dynamics in soil profiles by “Rock-Eval pyrolysis”: bulk characterization and quantification of degradation. *Eur. J. Soil Sci.* 57, 344–355. <https://doi.org/10.1111/j.1365-2389.2005.00745.x>.
- Simonneau, A., 2012. Empreintes climatiques et anthropiques sur le détritisme holocène: étude multiparamètres et intégrée de systèmes lacustres d’Europe de l’Ouest. Thèse de l’Université d’Orléans, p. 527.
- Simonneau, A., Chapron, E., Courp, T., Tachikawa, K., Le Roux, G., Baron, S., Galop, D., García, M., Di Giovanni, C., Motelica-Heino, M., Mazier, F., Foucher, A., Houet, T., Desmet, M., Bard, E., 2013a. Recent climatic and anthropogenic imprints on lacustrine systems in the Pyrenean Mountains inferred from minerogenic and organic clastic supply (Vicdessos valley, Pyrenees, France). *The Holocene* 23, 1764–1777.
- Simonneau, A., Chapron, E., Garçon, M., Winiarski, T., Graz, Y., Chauvel, C., Debret, M., Motelica-Heino, M., Desmet, M., Di Giovanni, C., 2014. Tracking Holocene glacial and high-altitude alpine environments fluctuations from minerogenic and organic markers in proglacial lake sediments (Lake Blanc Huez, Western French Alps). *Quat. Sci. Rev.* 89, 27–43.
- Simonneau, A., Doyen, E., Chapron, E., Millet, L., Vannière, B., Di Giovanni, C., Bossard, N., Tachikawa, K., Bard, E., Albéric, P., Desmet, M., Roux, G., Lajeunesse, P., Berger, J.F., Arnaud, F., 2013b. Holocene land-use evolution and associated soil erosion in the French Prealps inferred from Lake Paladru sediments and archaeological evidences. *J. Archaeol. Sci.* 40, 1636–1645. <https://doi.org/10.1016/j.jas.2012.12.002>.
- Stebich, M., Brückmann, C., Kulbe, T., Negendank, J.F.W., 2005. Vegetation history, human impact and climate change during the last 700 years recorded in annually laminated sediments of Lac Pavin, France. *Rev. Palaeobot. Palynol.* 133, 115–133. <https://doi.org/10.1016/j.revpalbo.2004.09.004>.
- Surmely, F., Miras, Y., Guenet, P., Nicolas, V., Savignat, A., Vannière, B., Walter-Simonnet, A.-V., Servera, G., Tzortzis, S., 2009. Occupation and land-use history of a medium mountain from the Mid-Holocene: a multidisciplinary study performed in the South Cantal (French Massif Central). *Comptes Rendus Palevol* 8, 737–748. <https://doi.org/10.1016/j.crpv.2009.07.002>.
- Syvitski, J.M.P., Milliman, J.D., 2007. Geology, geography, and humans battle for dominance over the delivery of fluvial sediment to the coastal ocean. *J. Geol.* 115, 1–19.
- Thouret, J.-C., Boivin, P., Labazuy, P., Leclerc, A., 2016. Geology, geomorphology and slope instability of the maar Lake Pavin (Auvergne, French Massif central). In: Sime- Ngando, T., Boivin, P., Chapron, E., Jézéquel, D., Meybeck, M. (Eds.), *Lake Pavin: History, Geology, Biogeochemistry and Sedimentology of a Deep Meromictic Maar Lake*. Springer Switzerland, Cham, pp. 155–174.
- Vanmaercke, M., Maetens, W., Poesen, J., Jankauskas, B., Jankauskiene, G., Verstraeten, G., de Vente, J., 2012. A comparison of measured catchment sediment yields with measured and predicted hillslope erosion rates in Europe. *J. Soils Sediments* 12, 586–602.
- Verheijen, F.G.A., Jones, R.J.A., Rickson, R.J., Smith, C.J., 2009. Tolerable versus actual soil erosion rates in Europe. *Earth Sci. Rev.* 94, 23–38. <https://doi.org/10.1016/j.earscirev.2009.02.003>.
- Verstraeten, G., Poesen, J., 2002. Using sediment deposits in small ponds to quantify sediment yield from small catchments: possibilities and limitations. *Earth Surf. Process. Landforms* 27, 1425–1439. <https://doi.org/10.1002/esp.439>.
- Walling, D.E., 1983. The sediment delivery problem. *J. Hydrol.* 65, 29–37.
- Yang, D.W., Kanae, S., Oki, T., Koike, T., Musiak, K., 2003. Global potential soil erosion with reference to land use and climate changes. *Hydrol. Process.* 17, 2913–2928.
- Zocatelli, R., Lavrieux, M., Guillemot, T., Chassiot, L., Le Milbeau, C., Jacob, J., 2017. Fecal biomarker imprints as indicators of past human land uses: source distinction and preservation potential in archaeological and natural archives. *J. Archaeol. Sci.* 81, 79–89. <https://doi.org/10.1016/j.jas.2017.03.010>.
- Zolitschka, B., 1998. A 14,000 year sediment yield record from western Germany based on annually laminated lake sediments. *Geomorphology* 22, 1–17.